

See discussions, stats, and author profiles for this publication at: <https://www.researchgate.net/publication/221742561>

The Aerobic Oxidation of a Pd(II) Dimethyl Complex Leads to Selective Ethane Elimination from a Pd(III) Intermediate

ARTICLE in JOURNAL OF THE AMERICAN CHEMICAL SOCIETY · FEBRUARY 2012

Impact Factor: 12.11 · DOI: 10.1021/ja210841f · Source: PubMed

CITATIONS

40

READS

31

3 AUTHORS:



[Julia Khusnutdinova](#)

Okinawa Institute of Science and Technology

26 PUBLICATIONS 515 CITATIONS

SEE PROFILE



[Nigam P Rath](#)

University of Missouri - St. Louis

529 PUBLICATIONS 6,941 CITATIONS

SEE PROFILE



[Liviu M Mirica](#)

Washington University in St. Louis

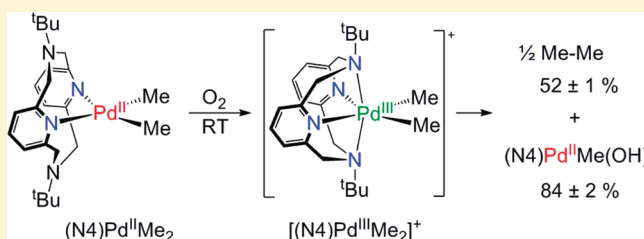
45 PUBLICATIONS 1,972 CITATIONS

SEE PROFILE

The Aerobic Oxidation of a Pd(II) Dimethyl Complex Leads to Selective Ethane Elimination from a Pd(III) Intermediate

Julia R. Khusnutdinova,[†] Nigam P. Rath,[‡] and Liviu M. Mirica^{*,†}[†]Department of Chemistry, Washington University, One Brookings Drive, St. Louis, Missouri 63130-4899, United States[‡]Department of Chemistry and Biochemistry, One University Boulevard, University of Missouri—St. Louis, Missouri 63121-4400, United States**S** Supporting Information

ABSTRACT: Oxidation of the Pd^{II} complex (N4)Pd^{II}Me₂ (N4 = *N,N'*-di-*tert*-butyl-2,11-diaza[3.3](2,6)pyridinophane) with O₂ or ROOH (R = H, *tert*-butyl, cumyl) produces the Pd^{III} species [(N4)Pd^{III}Me₂]⁺, followed by selective formation of ethane and the monomethyl complex (N4)Pd^{II}Me(OH). Cyclic voltammetry studies and use of 5,5-dimethyl-1-pyrroline-*N*-oxide (DMPO) as a spin trap suggest an inner-sphere mechanism for (N4)Pd^{II}Me₂ oxidation by O₂ to generate a Pd^{III}-superoxide intermediate. In addition, reaction of (N4)-Pd^{II}Me₂ with cumene hydroperoxide involves a heterolytic O–O bond cleavage, implying a two-electron oxidation of the Pd^{II} precursor and formation of a transient Pd^{IV} intermediate. Mechanistic studies of the C–C bond formation steps and crossover experiments are consistent with a nonradical mechanism that involves methyl group transfer and transient formation of a Pd^{IV} species. Moreover, the (N4)Pd^{II}Me(OH) complex formed upon ethane elimination reacts with weakly acidic C–H bonds of acetone and terminal alkynes, leading to formation of a new Pd^{II}–C bond. Overall, this study represents the first example of C–C bond formation upon aerobic oxidation of a Pd^{II} dimethyl complex, with implications in the development of Pd catalysts for aerobic oxidative coupling of C–H bonds.



INTRODUCTION

Palladium-catalyzed C–C coupling reactions are among the most important transformations in synthetic organic chemistry.¹ The vast majority of these reactions involve a C–C bond formation step at a Pd^{II} center to generate a Pd⁰ species which is subsequently reoxidized by a functionalized substrate,² a sacrificial oxidant,³ or even O₂.⁴ In addition, oxidative C–H coupling reactions have recently been reported in which the oxidation of an organometallic Pd^{II} species generates high-valent Pd^{III} or Pd^{IV} intermediates that undergo facile reductive elimination and C–C bond formation.^{5,6} However, the use of expensive and hazardous strong oxidants required to produce such high-valent Pd species limits the practical applications of these transformations.⁷ In this context, the development of oxidative C–H coupling reactions using molecular oxygen as an environmentally friendly and inexpensive oxidant is highly desirable.⁴

While various oxidants have been employed in the C–C coupling reactions catalyzed by high-valent Pd species,^{5,7} no C–C bond formation reactions induced by aerobic oxidation of Pd^{II} precursors have been reported to date. For example, C–C bond formation and ethane elimination from Pd^{II} dimethyl complexes have recently been shown to be induced by chemical oxidation through the intermediacy of high-valent Pd species.⁸ However, examples of aerobic oxidation Pd^{II} complexes leading to formation of detectable Pd^{III} or Pd^{IV} species are very rare.^{9,10} Moreover, while the intermediacy of Pd^{III} or Pd^{IV} species has

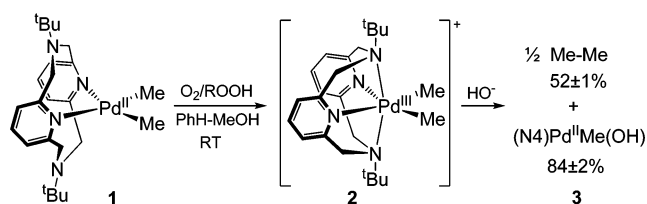
been recently proposed in some stoichiometric and catalytic aerobic oxidation reactions mediated by Pd^{II} complexes, no such species have been detected experimentally.^{11,12}

We have recently reported the one-electron oxidation of Pd^{II} precursors to yield stable Pd^{III} dimethyl and monomethyl species [(N4)Pd^{III}Me(X)]⁺ (X = Me, Cl; N4 = *N,N'*-di-*tert*-butyl-2,11-diaza[3.3](2,6)pyridinophane) that undergo light-induced elimination of ethane.¹³ Herein we report the facile oxidation of (N4)Pd^{II}Me₂ with O₂ or peroxides to form the Pd^{III} species [(N4)Pd^{III}Me₂]⁺, followed by selective formation of ethane and the monomethyl complex (N4)Pd^{II}Me(OH) (Scheme 1). Moreover, the latter product can further react and activate the weakly acidic C–H bonds of organic substrates such as acetone or terminal alkynes, leading us to propose a possible catalytic cycle that can be employed for the aerobic oxidative coupling of C–H bonds (*vide infra*). Cyclic voltammetry studies and spin trapping experiments with 5,5-dimethyl-1-pyrroline-*N*-oxide (DMPO) suggest an inner-sphere oxidation of (N4)Pd^{II}Me₂ by O₂ to generate a Pd^{III}-superoxide intermediate. In addition, oxidation of (N4)Pd^{II}Me₂ by cumene hydroperoxide leads to heterolytic O–O bond cleavage, implying a two-electron oxidation and formation of a transient Pd^{IV} intermediate. Mechanistic studies and crossover experiments of the C–C bond formation reaction are

Received: November 17, 2011

Published: December 22, 2011

Scheme 1. Oxidative C–C Bond Formation Reactivity of (N4)Pd^{II}Me₂ (1) in the Presence of O₂ or Peroxides



consistent with a nonradical mechanism that involves formation of a Pd^{IV} transient species. Overall, this study represents the first example of C–C bond formation upon aerobic oxidation of a Pd^{II} dimethyl complex, with direct implications in the development of Pd catalysts for the oxidative coupling of C–H bonds. These results suggest that generation of a Pd^{III} intermediate promotes the aerobic oxidation of the Pd^{II} precursor through an inner-sphere reduction of O₂, while transient formation of Pd^{IV} species is needed for a facile C–C bond formation.

EXPERIMENTAL DETAILS

General Specifications. All manipulations were carried out under a nitrogen atmosphere using standard Schlenk and glovebox techniques if not indicated otherwise. All reagents for which the synthesis is not given were commercially available from Aldrich, Acros, STREM, or Pressure Chemical, and were used as received without further purification. Solvents were purified prior to use by passing through a column of activated alumina using an MBRAUN SPS. N,N'-Di-*tert*-butyl-2,11-diaza[3.3](2,6)pyridinophane (N4),¹⁴ (COD)-Pd^{II}Cl₂,¹⁵ (N4)Pd^{II}Me₂ (1),¹³ [(N4)Pd^{III}Me₂]ClO₄ (2[ClO₄]),¹³ and (N4)Pd^{II}MeCl¹⁶ were prepared according to literature procedures. ¹H (300.121 MHz) NMR spectra were recorded on a Varian Mercury-300 spectrometer. ¹³C (151 MHz) NMR spectra were recorded on a Varian Unity Inova-600 spectrometer. UV–vis spectra were recorded on a Varian Cary 50 Bio spectrophotometer and are reported as λ_{max}/nm (ε, M^{−1} cm^{−1}). EPR spectra were recorded on a JEOL JES-FA X-band (9.2 GHz) EPR spectrometer at 77 or 298 K. ESI-MS experiments were performed using a Thermo FT or Bruker Maxis Q-TOF mass spectrometer with an electrospray ionization source. Elemental analyses were carried out by the Columbia Analytical Services Tucson Laboratory. Cyclic voltammetry experiments were performed with a BASi EC Epsilon electrochemical workstation or a CHI 660D Electrochemical Analyzer. Electrochemical-grade Bu₄NBF₄ (Fluka) was used as the supporting electrolyte. Electrochemical measurements were performed under a blanket of nitrogen, and the analyzed solutions were deaerated by purging with nitrogen. A glassy carbon disk electrode (*d* = 1.6 mm) and a Ag/0.01 M AgNO₃/MeCN electrode were used as the working and reference electrode, respectively. The nonaqueous reference electrode was calibrated against Cp₂Fe (Fc).

General Procedure for Oxidation of 1 with O₂ (or Peroxides). A 6.8 mM solution of 1 in O₂-saturated C₆D₆ was placed into an NMR tube and 1,3,5-trimethoxybenzene was added as an internal standard. The NMR tube was filled to the top (to avoid the escape of volatiles into the headspace) by addition of 1.2 mL of O₂-saturated CD₃OD and sealed with a septum. The concentration of 1 in the resulting solution is 3.4 mM. The reaction mixture was kept in the dark and periodically analyzed by ¹H NMR. The yield of the products were determined by NMR integration using 1,3,5-trimethoxybenzene as an internal standard, calculated as [moles of product]/[moles of 1] × 100%, and reported as the average of two runs. For oxidation with peroxides, all solutions were prepared in degassed solvents under N₂ atmosphere, and CD₃OD stock solutions of H₂O₂, ^{*t*}BuOOH, or cumyl peroxide were added to the reaction mixtures. For crossover experiments, a 1:1 mixture of 1 (13 μmol) and (N4)Pd(CD₃)₂⁺ 1-*d*₆ (13 μmol) was used.

UV–Vis Study of Formation of 2 during Oxidation of 1 with O₂ or Peroxides. A 1 mL solution of 1 (4.7 mM) in C₆H₆ was placed into a quartz cuvette (10 mm path length) equipped with a septum-sealed cap and a magnetic stir bar, and 1 mL of MeOH was added. O₂ was then bubbled through the solution for 10–15 min, and the reaction mixture was stirred under O₂ in the dark and the reaction progress was monitored by UV–vis. For reaction with peroxides, the reaction solution was prepared in degassed solvents under N₂ and a stock solution of peroxide in MeOH was added through the septum. The concentration of 2 during the reaction was calculated based on the extinction coefficient of the 750 nm absorption band (ε = 639 M^{−1} cm^{−1} in PhH-MeOH).

DMPO Spin Trap Experiments. A 8.9 mM stock solution of 1 in C₆H₆ and a 90 mM DMPO stock solution in MeOH were prepared in degassed solvents under N₂ and used immediately after preparation. Then 250 μL of the stock solution of 1 in C₆H₆ and 250 μL of the stock solution of DMPO in MeOH were combined in a vial equipped with a septum ([1] = 4.5 mM, [DMPO] = 45 mM). O₂ was bubbled through the solution for 1 min, and the solution was transferred to an EPR tube. The EPR spectrum was recorded immediately after preparation at 293 K.

General Procedure for NMR Studies of Reactivity of 2 with NaOD and Other Additives. A 2.37 mM solution of [2]ClO₄ in CD₃OD was prepared under a N₂ atmosphere, placed into an NMR tube, and 1,3,5-trimethoxybenzene was added as an internal standard. The NMR tube was filled to the top with 2.4 mL of the resulting solution (to avoid the escape of volatiles into the headspace), sealed with a septum, and then 1 equiv of a CD₃OD stock solution of NaOD or other additives was added. The reaction mixture was kept in the dark and periodically analyzed by ¹H NMR. The yield of the products were determined by NMR integration using 1,3,5-trimethoxybenzene as an internal standard, calculated as [moles of product]/[moles of 1] × 100%, and reported as the average of two runs. For crossover experiments, a 1:1 mixture of [2]ClO₄ and [(N4)Pd(CD₃)₂]⁺ 2-*d*₆ClO₄ was used.

General Procedure for Electrochemical Studies of 1 and 2. A solution of 1 in 0.1 M Bu₄NBF₄ 1:3 PhH-MeOH was deaerated by bubbling N₂ for 10–15 min and the cyclic voltammogram (CV) was recorded under a N₂ blanket. The 1:3 PhH-MeOH solvent mixture was used due its higher conductivity; however, similar results were obtained in 1:1 PhH-MeOH. O₂ was bubbled through the solution of 1 for 10 min, and cyclic voltammograms were then recorded under a blanket of O₂. Similarly, the CV of [2]ClO₄ was recorded in 0.1 M Bu₄NBF₄/PhH-MeOH under a blanket of O₂. As a control experiment, the CV of the O₂-saturated 0.1 M Bu₄NBF₄ 1:3 PhH-MeOH solution was recorded.

X-ray Structure Determination of 1, 2[ClO₄], 4[OTf], 5, and 6. Suitable crystals were mounted on Mitgen cryoloops in random orientations in a Bruker Kappa Apex-II CCD X-ray diffractometer equipped with an Oxford Cryostream LT device and a fine focus Mo Kα radiation X-ray source (λ = 0.71073 Å). Preliminary unit cell constants were determined with a set of 36 narrow frame scans. Typical data sets consist of combinations of φ and ψ scan frames with a typical scan width of 0.5° and a counting time of 15–30 s/frame at a crystal-to-detector distance of 3.5 cm. The collected frames were integrated using an orientation matrix determined from the narrow frame scans. Apex II and SAINT software packages (Bruker Analytical X-Ray, Madison, WI, 2008) were used for data collection and data integration. Analysis of the integrated data did not show any decay. Final cell constants were determined by global refinement of xyz centroids of reflections from the complete data sets. Collected data were corrected for systematic errors using SADABS (Bruker Analytical X-Ray, Madison, WI, 2008) based on the Laue symmetry using equivalent reflections. Crystal data and intensity data collection parameters are listed in Tables S8–15. Structure solutions and refinement were carried out using the SHELXTL-PLUS software package (see the Supporting Information). The structures were solved by direct methods and refined successfully in the C2/c, C2/c, P-1, P-1, and Cc space groups, respectively. Full matrix least-squares refinements were carried out by minimizing Σw(F_o² − F_c²)². The non-hydrogen

atoms were refined anisotropically to convergence. The hydrogen atoms were treated using appropriate riding model (AFIX m3).

RESULTS AND DISCUSSION

Characterization and Oxidation Studies of (N4)-Pd^{II}Me₂ (1). The dimethyl complex (N4)Pd^{II}Me₂, **1**, was synthesized according to a previously published method¹³ and was characterized by X-ray diffraction (Figure 1a). The X-ray

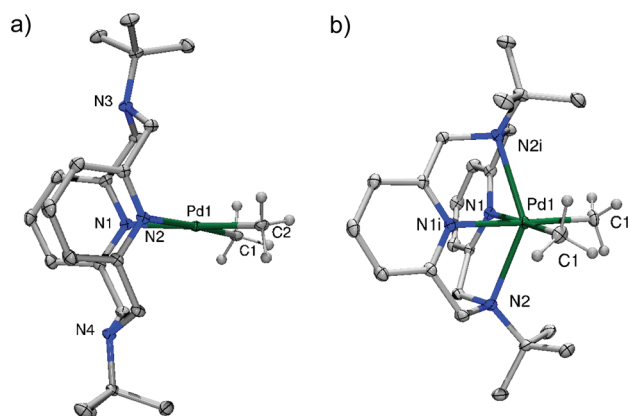


Figure 1. ORTEP representation of **1** (a) and the cation of **2**[ClO₄] (b). Selected bond lengths (Å), **1**: Pd1–C1 2.099; Pd1–C2 2.099; Pd1–N1 2.173; Pd1–N2 2.173. **2**: Pd1–C1 2.048; Pd1–C1i 2.048; Pd1–N1 2.112; Pd1–N1i 2.112; Pd1–N2 2.469; Pd1–N2i 2.469.

structure of **1** reveals a square planar geometry around the Pd^{II} center with the N4 ligand bound through the two pyridyl N atoms, whereas the two amine donors are pointing away from the metal center. The cyclic voltammogram (CV) of **1** in 0.1 M Bu₄NBF₄/THF exhibits a Pd^{II}/III oxidation peak potential at –0.36 V vs Fc⁺/Fc¹³ that is significantly lower than the oxidation potentials of Pd^{II}Me₂ complexes supported by bidentate N-donor ligands.^{8,17} For example, complexes (tmeda)Pd^{II}Me₂ and (tBu₂bipy)Pd^{II}Me₂ exhibit irreversible oxidation waves at +0.30 V and +0.45 V vs Fc⁺/Fc, respectively (Figures S30 and S31).¹⁷ The uncommonly low oxidation potential of **1** is due to the ability of the tetradentate ligand N4 to form (κ³-N4)PdMe₂ or (κ⁴-N4)PdMe₂ species¹⁸ that have lower oxidation potentials,^{19–21} as well as stabilize the distorted octahedral geometry of the Pd^{III} center (Figure 1b).¹³ Such a low oxidation potential of **1** has prompted us to study its reactivity toward O₂. While solutions of **1** in aprotic solvents such as benzene, toluene, fluorobenzene, or THF are stable under 1 atm O₂ for several days, the addition of methanol to a solution of **1** in any of these solvents leads to the formation of a green paramagnetic species identified as [(N4)Pd^{III}Me₂]⁺, **2**, which exhibits an UV–vis spectrum identical to that of the independently synthesized 2[ClO₄] complex (Figure 2).¹³ Interestingly, the EPR spectrum of **2** in frozen MeOH (or in a glassing solvent mixture)¹⁷ reveals superhyperfine coupling to two N atoms in both parallel and perpendicular directions (Figure 3),^{9,22a} which is different from the broad EPR spectrum observed in MeCN.¹³ This difference is likely due to a more symmetric structure of **2** in a frozen protic solvent that results in sharper EPR features and a larger separation between the g_z and g_x/g_y values.^{9,22b} In addition, the presence of a dynamic Jahn–Teller distortion in frozen MeCN at 77 K can also lead to a broader EPR spectrum.²³ Indirect support for this behavior in frozen solution is provided by the solid-state C₂ symmetric

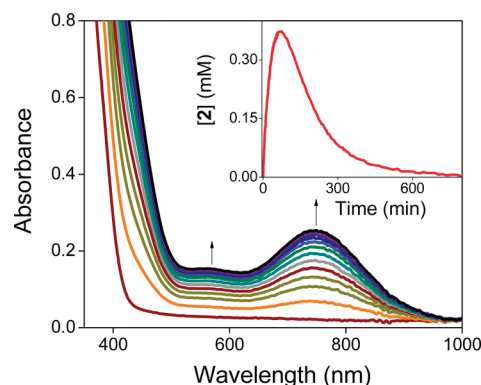


Figure 2. Formation of **2** during aerobic oxidation of **1** (2.3 mM) in 1:1 PhH–MeOH followed by UV–vis spectroscopy ($\Delta t = 4.5$ min, $t_{\text{max}} = 70$ min). Inset: plot of the concentration of **2** during oxidation of **1** under the same conditions.

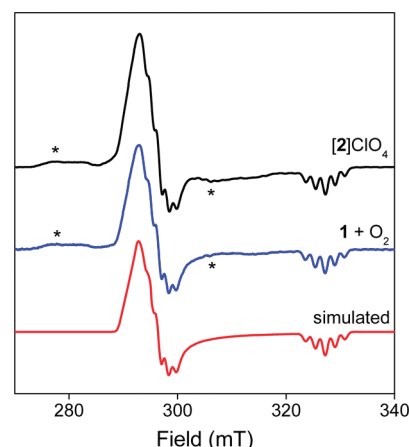


Figure 3. EPR spectra of 0.7 mM solution of [2]ClO₄ in MeOH (black line), the product of oxidation of **1** (4.5 mM) with O₂ in 1:1 PhH–MeOH, and a simulated EPR spectrum (red line) using the following parameters: g_x = 2.221 (A_N = 12.0 G); g_y = 2.191 (A_N = 13.8 G); g_z = 1.986 (A_N = 18.0 G). The features marked with an asterisk are due to the hyperfine coupling to the ¹⁰⁵Pd isotope (abundance 22.3%, I = 5/2).

structure of 2[ClO₄] crystallized from MeOH (Figure 1b), as opposed to the C₁ symmetric structure obtained from MeCN.¹³ Formation of the [(N4)Pd^{III}Me₂]⁺ species was also confirmed by the ESI-MS of an O₂-saturated MeOH solution of **1** that reveals a peak at *m/z* 488.2118 amu (calcd for **2**: 488.2131 amu). Moreover, the maximum yield of **2** observed during aerobic oxidation increases with increasing concentrations of MeOH in solution. Stirring a solution of **1** in 1:3 PhH–MeOH under 1 atm O₂ for 60 min generates **2** in 26% yield, whereas the maximum yield of **2** is only 16% in 1:1 PhH–MeOH. Formation of **2** was also observed in solution mixtures containing other protic solvents such as acetone–water and THF–water (Table S8).¹⁷ Overall, we propose that the presence of protons is needed to facilitate the irreversible reduction of O₂ along with the oxidation of **1** to **2**, in a mechanism similar to that proposed for the aerobic oxidation of Pt^{II}Me₂ complexes in protic solvents (vide infra).^{21,24,25} As **1** is poorly soluble in neat MeOH or water-containing solvent mixtures, a 1:1 PhH–MeOH (v:v) solvent mixture was used for further studies as it provides an optimal solubility for both **1** and **2**.

The UV–vis spectra obtained during the reaction of **1** with O_2 in 1:1 PhH–MeOH show that the concentration of **2** increases rapidly during the initial period of time (~ 70 min) and then slowly decays over the course of several hours (Figure 2, inset). When the oxidation of **1** in O_2 -saturated 1:1 C_6D_6 – CD_3OD is monitored by 1H NMR spectroscopy, the formation of ethane and a new diamagnetic Pd^{II} complex is detected in $52 \pm 1\%$ and $84 \pm 2\%$ yields, respectively, after 8 h at RT (a theoretical yield of 50% ethane is expected based on the reaction shown in Scheme 1).^{8,13} The Pd^{II} complex formed upon ethane elimination was identified as the Pd^{II} methyl hydroxo complex $(N4)Pd^{II}Me(OH)$, **3** (vide infra).²⁶

A similar oxidation reactivity was observed when **1** was reacted with oxidants such as H_2O_2 , $tBuOOH$, or cumene hydroperoxide (CumOOH). For example, the oxidation of **1** with 1 equiv of H_2O_2 in 1:1 PhH–MeOH generates **2** in 41% yield after 10 min, as detected by UV–vis and EPR spectroscopy, followed by its slow decay. 1H NMR analysis of the reaction of **1** with 1 equiv H_2O_2 in 1:1 C_6D_6 – CD_3OD reveals the formation of ethane and **3** in $46 \pm 1\%$ and $60 \pm 3\%$ yield, respectively. Similarly, the oxidation of **1** with 1 equiv $tBuOOH$ in 1:1 C_6D_6 – CD_3OD produces ethane and **3** in $43 \pm 1\%$ and $78 \pm 1\%$ yield, respectively. The oxidation of **1** with 0.5 equiv of H_2O_2 or $tBuOOH$ leads to formation of ethane in similar yields to the use of 1 equiv oxidant, suggesting a 1:peroxide stoichiometry of 2:1. For example, oxidation of **1** with 0.5 equiv of H_2O_2 or $tBuOOH$ leads to the formation of ethane in $42 \pm 1\%$ and $40 \pm 2\%$ yields, respectively (Tables S3 and S4). Overall, these results suggest that both O_2 and peroxides are capable of oxidizing **1** to **2**, which is likely intimately involved in the observed C–C bond formation (vide infra).¹³

Mechanistic Studies of the Oxidation of 1. Formation of **2** from **1** and O_2 is intriguing since, while there are several reports on the oxidation of Pd^0 complexes by O_2 ,²⁷ only a few Pd^I and Pd^{II} complexes^{11,28} have been shown to react with O_2 , and only two systems lead to formation of detectable Pd^{III} species.^{9,10} However, the mechanism of aerobic oxidation in these latter systems has not been investigated. To obtain further insight into the oxidation of $(N4)Pd^{II}Me_2$, we first considered the in situ formation of H_2O_2 from MeOH and O_2 in the presence of **1**, given the previous reports of Pd^{II} -catalyzed H_2O_2 formation through aerobic oxidation of primary and secondary alcohols.²⁹ However, no H_2O_2 was detected at levels above 2 μM (i.e., $<0.1\%$) in a 2.2 mM solution of **1** in 1:1 THF–MeOH using an Amplex red/horseradish peroxidase (HRP) assay.¹⁷ Moreover, formation of Pd black was not observed during the reaction of **1** with O_2 .³⁰ The formation of Pd^{III} species was also observed by UV–vis and EPR in benzene in the presence of proton donors such as phenol or acetic acid.¹⁷ These results indicate that MeOH likely acts as a mildly acidic source of protons that promotes the aerobic oxidation of **1** and not as a sacrificial reductant.³⁰

Cyclic Voltammetry Studies of O_2 Reduction in the Presence of 1. The possibility of an outer-sphere electron transfer from **1** to O_2 to form **2** and superoxide ($O_2^{\bullet-}$) also needs to be considered. Cyclic voltammetry (CV) studies reveal that the Pd^{II}/Pd^{III} oxidation wave potential is ~ 0.8 V more positive than the O_2 reduction peak potential, arguing against an outer-sphere electron transfer mechanism.¹⁷ Moreover, the CV of **1** (or **2**) in O_2 -saturated 1:3 PhH–MeOH reveals an O_2 reduction wave at a potential that is 0.5–0.6 V more positive than the O_2 reduction peak potential in the absence of the Pd

complex (Figure 4).^{17,31} The current of the O_2 reduction wave is significantly higher in the presence of **1** or **2** compared to the

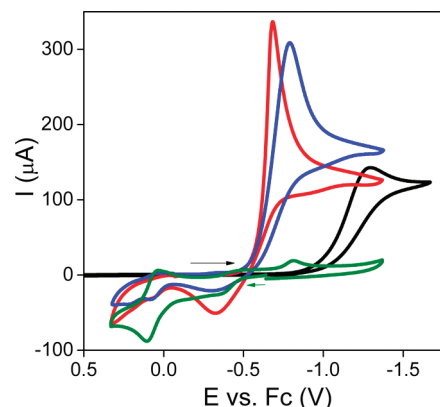
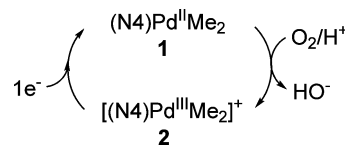


Figure 4. CVs in 1:3 PhH–MeOH, (scan rate 100 mV/s): O_2 reduction wave in absence of Pd complexes (black line); in presence of 2.2 mM **1** (red line); in presence of 2.2 mM $[2]ClO_4$ (blue line); CV of 2.2 mM **1** in absence of O_2 (green line, the I axis multiplied by $10\times$).

peak current of O_2 reduction in absence of Pd complexes (Figure 4), suggestive of an electrocatalytic O_2 reduction. The appearance of an O_2 reduction catalytic-like wave in the presence of **1** (or **2**) can be explained by an inner-sphere oxidation of **1** with O_2 to produce **2**, which is subsequently electrochemically reduced to **1** and thus completes an electrocatalytic cycle (Scheme 2). Similar electrocatalytic O_2

Scheme 2. Catalytic O_2 Electroreduction in the Presence of **1** or **2**



reduction has been observed in the presence of other transition metal complexes capable of an inner-sphere O_2 reduction.^{31,32}

DMPO Spin Trap Studies. Alternatively, O_2 could be involved in an inner-sphere oxidation of **1** to a $Pd^{III}-O_2^{\bullet-}$ species. To detect any oxygen-containing intermediate, the oxidation of **1** with O_2 was carried out in the presence of 5,5-dimethyl-1-pyrroline-N-oxide (DMPO), a commonly used spin trap for O-centered radicals.³³ When a solution of **1** (4.5 mM) and DMPO (45 mM) in 1:1 PhH–MeOH was reacted with O_2 , the EPR spectrum of the reaction mixture showed the formation of an unstable DMPO spin adduct that exhibits four broad lines ($A_N = 13.8$ G, $A_H = 9.9$ G, $g = 2.004$, Figure 5). These hyperfine coupling constants are typical for DMPO adducts of O-centered radicals, yet they are distinctly different from the hyperfine coupling constants characteristic for DMPO adducts of C-centered radicals, hydroxyl radical, or superoxide radical.³³ Similar broad features have been reported for the DMPO adducts of Co^{III} - and Cu^{II} -superoxide complexes formed during the oxidation of the corresponding precursors with O_2 in the presence of DMPO.^{34,35} Moreover, a similar DMPO adduct was observed when O_2 was reacted with a solution containing equimolar amounts of $Co(ClO_4)_2 \cdot 6H_2O$ and the ligand N4 in MeOH ($A_N = 13.6$ G, $A_H = 7.6$ G, $g =$

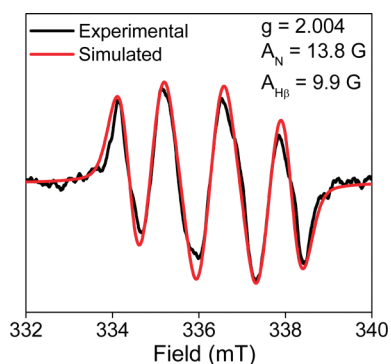
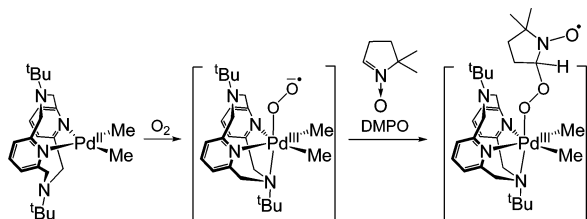


Figure 5. EPR spectrum of **1** (4.5 mM) in 1:1 PhH-MeOH in the presence of DMPO (45 mM), 2 min after exposure to O_2 .

2.005).¹⁷ Overall, these observations are suggestive of an inner-sphere oxidation of **1** by O_2 to form a proposed Pd^{III} -superoxide that is trapped by DMPO to form a Pd^{III} -peroxide-DMPO adduct (Scheme 3), similar to the one proposed for a Co complex.³⁴

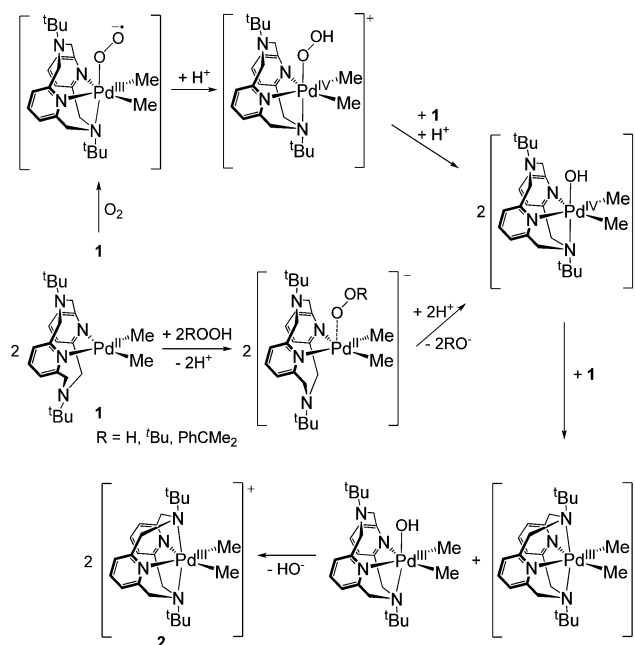
Scheme 3. Proposed Mechanism of Oxidation of **1** by O_2 and Formation of a DMPO Radical Adduct



Proposed Mechanisms for Oxidation of 1 with O_2 . In contrast to the dearth of Pd^{II} complexes that undergo aerobic oxidation, there are several reports of aerobic oxidation of analogous Pt organometallic complexes. For example, a number of Pt^{II} dimethyl complexes supported by bidentate or tridentate N-donor ligands have been reported to react with O_2 to generate Pt^{IV} complexes.^{21,24} The first steps of the reaction of **1** with O_2 can be viewed as similar to those proposed for the Pt^{II} complexes, in which the presence of a protic solvent may be required for the proton transfer to a transient Pt^{III} -superoxide complex to form high-valent Pt^{IV} -hydroperoxo²¹ and/or -hydroxo species (Scheme 4).^{21,24} Although no Pd^{IV} species has been detected by NMR in our reaction mixtures, $(N4)Pd^{IV}$ -hydroperoxo and/or -hydroxo intermediates can form transiently and undergo rapid comproportionation in the presence of $(N4)Pd^{II}$ complexes to yield a Pd^{III} species.⁹ Such comproportionation reaction was observed for an analogous system in which the electrochemically generated $[(N4)Pd^{IV}MeCl]^{2+}$ species reacts rapidly with 1 equiv $(N4)Pd^{II}MeCl$ to form 2 equiv of $[(N4)Pd^{III}MeCl]^+$ quantitatively.³⁶ Similarly, comproportionation of $[(\kappa^3-N4)-Pd^{IV}Me_2(OH)]^+$ and **1** would generate **2** and a $[(\kappa^3-N4)Pd^{III}Me_2(OH)]$ species, which can undergo an entropically favored displacement of the hydroxide ligand by the amine group²⁰ to stabilize the distorted octahedral Pd^{III} center and yield another molecule of **2** (Scheme 4).¹³

Proposed Mechanisms of Oxidation of 1 with Peroxides. The reaction of **1** with peroxides provides further insight into its oxidation mechanism. For example, cumene hydroperoxide (CumOOH) has been reported to react with transition metal

Scheme 4. Proposed Mechanisms of Formation of **2** during Oxidation of **1** by O_2 or Peroxides



complexes via either heterolytic or homolytic O–O bond cleavage leading to the formation of α -cumyl alcohol or a cumyloxy radical, respectively; the latter subsequently produces acetophenone as a major product via a methyl radical loss.³⁷ Reaction of **1** with 1 equiv CumOOH produces ethane and **3** in $40 \pm 1\%$ and $64 \pm 1\%$ yields, respectively. The reaction is accompanied by consumption of ~ 0.63 equiv CumOOH and formation of an equivalent amount of α -cumyl alcohol. No acetophenone was detected in the reaction mixture, suggestive of a heterolytic O–O bond cleavage and thus a two-electron oxidation of **1** by CumOOH.³⁷ Moreover, no DMPO adducts of hydroxyl radical or solvent-derived radicals were detected during the oxidation of **1** with 1 equiv of H_2O_2 , ruling out a Fenton-type radical mechanism.³⁸ This two-electron oxidation of the Pd^{II} center by the metal-bound peroxide would generate a Pd^{IV} -hydroxo³⁹ (or Pd^{IV} -oxo⁴⁰) intermediate, which can react with **1** to yield 2 equiv of the Pd^{III} species, consistent with the observed 1:cumene hydroperoxide stoichiometry of $\sim 2:1$ (Scheme 4).⁴¹ Overall, these mechanistic studies suggest the involvement of transient Pd^{IV} intermediates during the oxidation of **1**, although the steric properties of the N4 ligand preferentially stabilize the observed Pd^{III} complex **2**.

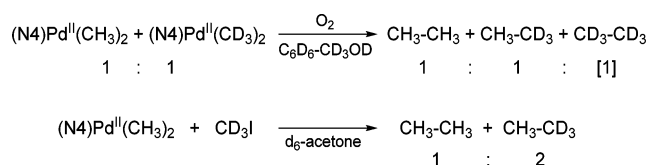
C–C Bond Formation Reactivity Studies of 2. Based on the reported light-induced elimination of ethane and a Pd^{II} monomethyl complex from the isolated Pd^{III} complex $2[ClO_4]$,¹³ we propose that the detected species **2** during oxidation of **1** is likely a reactive intermediate leading to C–C bond formation. When a CD_3OD solution of $[2]ClO_4$ was exposed to visible light in the absence of O_2 , ethane was formed in $44 \pm 1\%$ yield, along with **3** in $72 \pm 1\%$ yield (after addition of 1 equiv NaOH).¹⁷ However, the oxidation of **1** with O_2 or peroxide gives identical yields of ethane in the presence or absence of ambient light. To further study the reactivity of **2** in the dark, we investigated the effect of various additives on the stability of **2**. While **2** is stable in CD_3OD in the dark in the presence or absence of O_2 , the addition of 1 equiv NaOD leads to elimination of ethane and **3**.¹⁷ The reaction performed in

absence of O₂ gave ethane and 3 in 22% and 39% yield, respectively after 4 h, while the reaction performed under 1 atm O₂ yielded 41% of ethane after 4 h. The yield of ethane obtained in the latter case is similar to that observed under the typical conditions for aerobic oxidation of 1, suggesting that 2 is a viable reaction intermediate leading to ethane elimination. The yield of ethane remained unaffected when 2[ClO₄] reacted with 1 equiv NaOD in the presence of the radical traps such as TEMPO, suggesting a nonradical pathway for C–C bond formation. The absence of a radical mechanism leads us to propose a Me group transfer between two Pd^{III} species to give a transient Pd^{IV}Me₃ intermediate (vide infra).⁸ This is supported by the reaction of 1 with a two-electron oxidant MeI that leads to elimination of ethane and (N4)Pd^{III}MeI.¹³

The generation of hydroxide ions in solution likely results from the reduction of O₂ (or peroxides) in the presence of a protic solvent. Moreover, hydroxide is likely the counteranion for the cationic species 2 formed during oxidation of 1 with O₂ or peroxides, and also leads to the formation of the Pd^{III} methyl hydroxo complex 3 as a final product (vide infra). Overall, we propose that the reversible HO[−] binding to the Pd^{III} center through displacement of one axial amine group promotes the formation of a transient Pd^{IV} intermediate and the subsequent C–C bond elimination (vide infra). Similarly, the addition of other coordinating anions such as CN[−] or MeO[−] induces a similar ethane elimination reactivity of 2[ClO₄] in the dark.¹⁷

Crossover Experiments. To gain insight into the possible mechanism of ethane formation, crossover experiments were performed using a 1:1 mixture of (N4)Pd(CH₃)₂, 1, and (N4)Pd(CD₃)₂, 1-*d*₆ in C₆D₆-CD₃OD. The control experiment in absence of O₂ showed no scrambling between 1 and 1-*d*₆ in C₆D₆ or C₆D₆-CD₃OD solutions for at least 8 h, both in the presence or absence of ambient light. Oxidation of a 1:1 mixture of 1 and 1-*d*₆ with O₂ in 1:1 C₆D₆-CD₃OD leads to formation of CH₃CH₃ and CH₃CD₃ in 16.5% and 15% yields, respectively, after 8 h. Given the typical yield of ~50% ethane upon oxidation of 1, the yield of CD₃CD₃ can be estimated as ~18%, suggesting a nearly 1:1:1 ratio of CH₃CH₃:CH₃CD₃:CD₃CD₃ (Scheme 5, top). Similarly, the

Scheme 5. Crossover Experiment between 1 and 1-*d*₆ (top) and the Reaction of 1 with CD₃I (Bottom)



elimination of ethane from a 1:1 mixture of [(N4)Pd^{III}(CH₃)₂]-ClO₄, [2]ClO₄, and [(N4)Pd^{III}(CD₃)₂]-ClO₄, [2-*d*₆]ClO₄, in the presence of 1 equiv NaOD produces CH₃CH₃ and CH₃CD₃ in a 1:1 ratio after 24 h in the dark. The ESI-MS of the 1:1 mixture of [2]ClO₄ and [2-*d*₆]ClO₄ shows no methyl group scrambling after 8 h in the dark, suggesting that methyl group exchange does not occur at Pd^{III} centers on this time scale. Moreover, no scrambling was observed for the Pd^{III} complexes generated by aerobic oxidation of a 1:1 mixture of 1 and 1-*d*₆.¹⁷

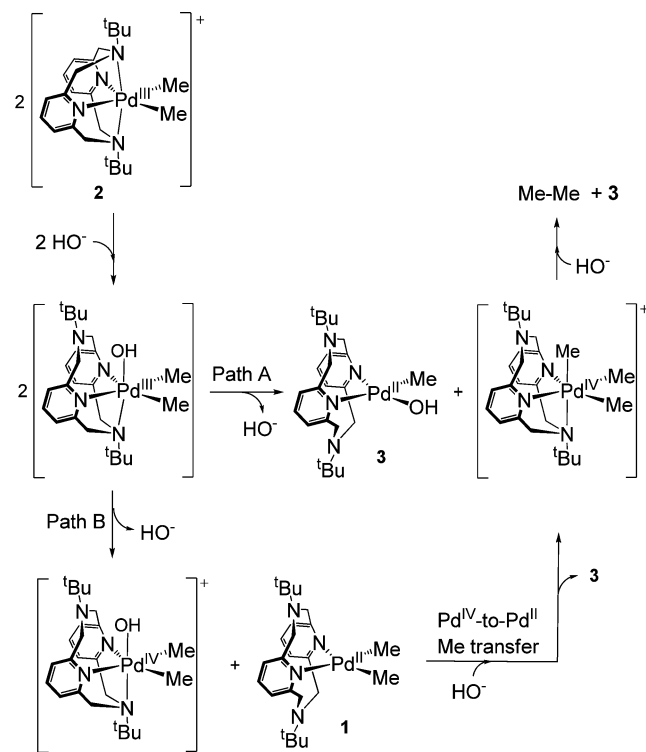
Proposed Mechanisms of Ethane Formation. The observed 1:1:1 ratio of ethane isotopomers rules out a radical mechanism of ethane formation involving Me radicals that would lead to the statistical 1:2:1 ratio of

CH₃CH₃:CH₃CD₃:CD₃CD₃.⁴² The observed 1:1:1 ratio is consistent with a mechanism involving a Me group transfer between two Pd^{III} dimethyl species to form a [(N4)Pd^{IV}Me₃]⁺ intermediate and a Pd^{II} monomethyl species. The formed [(N4)Pd^{IV}Me₃]⁺ species is expected to undergo fast rearrangement of the methyl groups and lead to reductive elimination of any two of the three Me groups.^{43,44} This proposed mechanism yields a 1:1:1 ratio of CH₃CH₃:CH₃CD₃:CD₃CD₃ for the crossover experiment (Scheme S1), in line with the experimental result.¹⁷

The rapid intramolecular rearrangement of the methyl groups in the proposed [(N4)Pd^{IV}Me₃]⁺ intermediate was confirmed by the reaction of (N4)Pd^{II}Me₂ with CD₃I, which yields CH₃CH₃ and CH₃CD₃ in a 1:2 ratio (Scheme 5, bottom).¹⁷ Similar results have been reported for the oxidative addition of CD₃I to the analogous (bpy)Pd^{II}(CH₃)₂ complex^{43,44} to form a (bpy)Pd^{IV}(CH₃)₂(CD₃)⁺ species that undergoes rapid rearrangement of the equatorial CH₃ and axial CD₃ groups to give a statistical mixture of isotopomeric Pd^{IV} complexes.^{43,44} Subsequent reductive elimination would lead to formation of CH₃CH₃ and CH₃CD₃ in a 1:2 ratio, similar to that observed for 1.

Our mechanistic studies suggest that ethane elimination is likely promoted by a coordinating anion such as HO[−], which displaces one of the amine groups and leads to a [(κ³-N4)Pd^{III}Me₂(OH)] complex. Since the increased stability of the (κ⁴-N4)Pd^{III} species is likely due to the ability of the N4 ligand to accommodate a distorted octahedral geometry of the Pd^{III} center,¹³ disruption of the κ⁴-coordination mode by HO[−] likely induces Me group transfer between two Pd^{III} species to generate [(κ³-N4)Pd^{IV}Me₃]⁺ and [(N4)Pd^{II}Me(OH)], 3 (Scheme 6, path A). Such reactivity has been observed

Scheme 6. Proposed Mechanisms for C–C Bond Formation



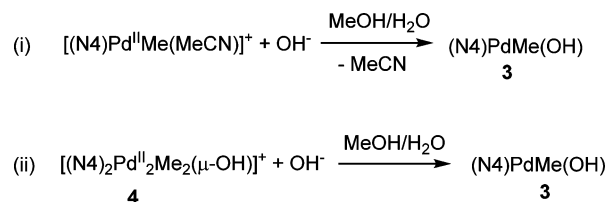
previously for Pd^{II} and Pt^{II} complexes supported by bidentate (or tridentate) ligands,⁴⁴ for which facile Me group transfer

reactions occur upon one-electron oxidation.^{8,45} Another possible mechanism may involve an initial disproportionation of $[(\kappa^3\text{-N4})\text{Pd}^{\text{III}}\text{Me}_2(\text{OH})]$ to generate $[(\kappa^3\text{-N4})\text{Pd}^{\text{IV}}\text{Me}_2(\text{OH})]^+$ and **1** (Scheme 6, path B). Subsequent Me group transfer from $[(\kappa^3\text{-N4})\text{Pd}^{\text{IV}}\text{Me}_2(\text{OH})]^+$ to **1** could generate **3** and $[(\kappa^3\text{-N4})\text{Pd}^{\text{IV}}\text{Me}_3]^+$, the latter species being responsible for ethane formation. A similar Me group transfer reaction from an electrophilic $\text{Pd}^{\text{IV}}\text{Me}_3$ center to a nucleophilic Pt^{II} center been reported previously.⁴⁶

Characterization and C–H Activation Reactivity of **3**.

The identity of a Pd^{II} methyl hydroxo complex **3** formed upon ethane elimination from **1** (Scheme 1) was confirmed by its independent synthesis from $(\text{N4})\text{Pd}^{\text{II}}\text{Me}(\text{MeCN})^+$ and 1 equiv OH^- (Scheme 7, eq (i)). Attempts to isolate **3** in the solid state

Scheme 7. Independent Syntheses of **3**



led to the formation of a dinuclear hydroxo-bridged complex $[(\text{N4})\text{Pd}^{\text{II}}\text{Me}(\mu\text{-OH})\text{Pd}^{\text{II}}\text{Me}(\text{N4})](\text{OTf})$, **4** $[\text{OTf}]$, which was characterized by X-ray diffraction (Figure 6). Both metal

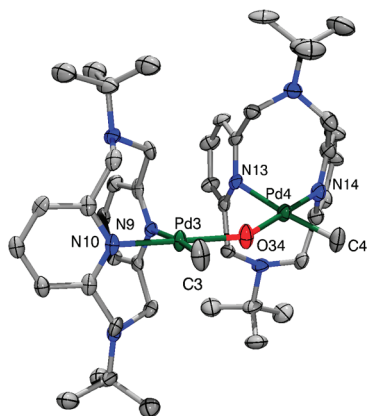


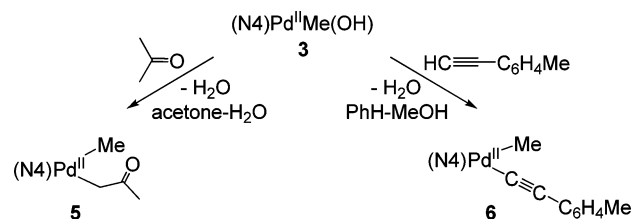
Figure 6. ORTEP representation of the cation of **4** $[\text{OTf}]$. Selected bond lengths (Å): Pd3–C3 2.018; Pd3–N10 2.029; Pd3–O34 2.034; Pd3–N9 2.180; Pd4–C4 2.010; Pd4–O34 2.033; Pd4–N14 2.056; Pd4–N13 2.183; Pd3...Pd4 3.832. Only one of the two conformers present in the crystal structure is shown.

centers in **4** exhibit a square planar geometry with each Pd^{II} atom surrounded by two pyridyl N atoms, one methyl group, and a bridging hydroxide ligand. Notably, there are only three other examples of structurally characterized dinuclear Pd complexes with a single bridging hydroxo ligand.^{47,48} Addition of 1 equiv OH^- to **4** in MeOH quantitatively generates **3** (Scheme 7, eq (ii)), whose ^1H NMR spectrum is identical to that of **3** obtained from $(\text{N4})\text{Pd}^{\text{II}}\text{Me}(\text{MeCN})^+$.¹⁷

Interestingly, when the aerobic oxidation of **1** was performed in 15:1 d_6 -acetone- D_2O , ethane formed in 40% yield after 8 days along with a new Pd^{II} product identified as the acetonyl complex $(\text{N4})\text{PdMe}(\text{CD}_2\text{COCOD}_3)$, **5**, obtained in 42% yield.¹⁷ The latter complex could be obtained upon deprotonation of acetone by the hydroxo ligand of **3**.⁴⁹ This was confirmed by

reacting independently prepared **3** with 3:1 acetone- CH_3OH to give **5** (Scheme 8), which was isolated in 46% yield and

Scheme 8. Reactivity of **3** with Acetone and 4-Ethynyltoluene



characterized by NMR spectroscopy and X-ray diffraction (Figure 7a).¹⁷ Similarly, **3** reacts with 4-ethynyltoluene to

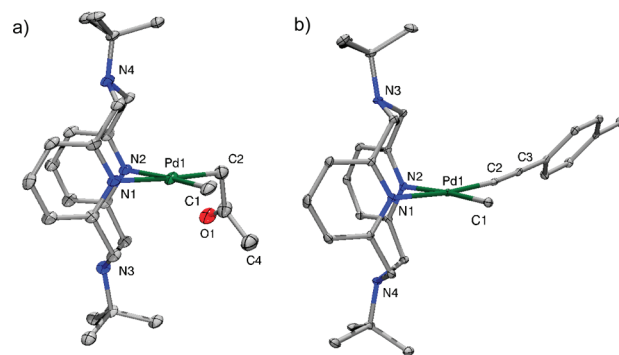
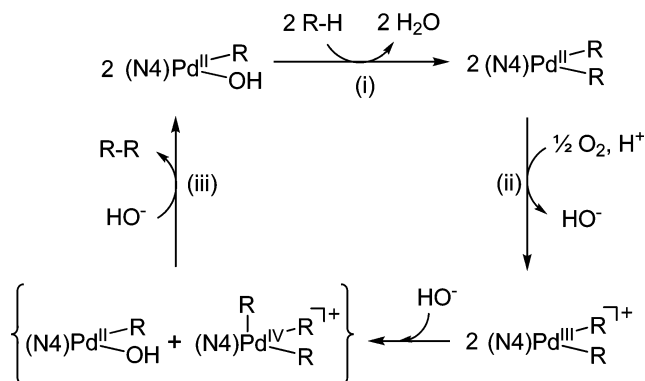


Figure 7. ORTEP representation of **5** (a) and **6** (b). Selected bond lengths (Å): **5**: Pd1–C1 2.020; Pd1–C2 2.046; Pd1–N1 2.125; Pd1–N2 2.196; **6**: Pd1–C1 2.032; Pd1–C2 1.959; Pd1–N1 2.107; Pd1–N2 2.144.

generate the corresponding acetylide complex $(\text{N4})\text{Pd}^{\text{II}}\text{Me}(\text{C}\equiv\text{CC}_6\text{H}_4\text{Me})$, **6**, which was isolated and structurally characterized (Figure 7b).¹⁷ The observed reactivity demonstrates the ability of **3** to activate substrates containing weakly acidic C–H bonds and form a new Pd–C bond.⁴⁹ Interestingly, although complex **5** does not react with O_2 or peroxides, its oxidation can be accomplished using Fc^+ to produce a Pd^{III} species that was characterized by UV–vis and EPR (Figure S27),¹⁷ suggesting that a range of organometallic $(\text{N4})\text{Pd}^{\text{II}}$ complexes could be oxidized to Pd^{III} intermediates and possibly be involved in a catalytic oxidative coupling of C–H bonds (vide infra).

Proposed Catalytic Cycle for the Aerobic Oxidative Coupling of C–H Bonds. Based on the observed reactivity of $(\text{N4})\text{Pd}$ -methyl complexes in aerobic oxidation, C–C bond formation, and C–H bond activation reactions, we propose a catalytic cycle for the oxidative coupling of C–H bonds using O_2 as the oxidant (Scheme 9).⁵⁰ In this catalytic cycle, a monohydrocarbyl hydroxo complex $(\text{N4})\text{Pd}^{\text{II}}\text{R}(\text{OH})$ activates the C–H bond of an organic substrate to give a bis-(hydrocarbyl) species $(\text{N4})\text{Pd}^{\text{II}}\text{R}_2$ (Scheme 9, step (i)). The ability of hydroxo complexes of late transition metals to activate C–H bonds has been previously reported.^{47,49,51} The resulting $(\text{N4})\text{Pd}^{\text{II}}\text{R}_2$ species is expected to have a low oxidation potential and react with O_2 to form a $[(\text{N4})\text{Pd}^{\text{III}}\text{R}_2]^+$ intermediate (Scheme 9, step (ii)). Subsequent C–C bond formation through the intermediacy of a $\text{Pd}^{\text{IV}}\text{R}_3$ species would lead to the coupled product and regeneration of a

Scheme 9. Proposed Catalytic Cycle for the Aerobic Oxidative Coupling of C–H Bonds That Involves (i) C–H Bond Activation, (ii) Aerobic Pd^{II} Oxidation, and (iii) C–C Bond Formation



monohydrocarbyl complex (N4)Pd^{III}R(OH) (Scheme 9, step (iii)).

Such a direct oxidative coupling of C–H bonds is currently of great practical interest in the chemical industry. For example, the oxidative coupling of methane into higher hydrocarbons can provide a means of converting abundant natural gas resources into useful chemicals.⁵² However, the utilization of molecular oxygen as the oxidant in these C–H coupling reactions remains a challenge.⁴ We have demonstrated herein the viability of all three steps of the proposed catalytic cycle for Pd complexes supported by the tetradentate ligand N4. Further studies will be directed toward the development of metal complexes capable of catalytic aerobic transformations. Our results strongly suggest that stabilization of a Pd^{III} species promotes the aerobic oxidation of Pd^{II} precursors, while formation of Pd^{IV} intermediates is needed for an efficient C–C bond formation. As such, the ability of N4 or other tetradentate ligands to access both high-valent Pd species may be necessary to promote efficient aerobic C–H coupling reactions.

CONCLUSION

In summary, reported herein is the first example of an aerobic oxidation of a Pd^{II} dimethyl complex that leads to selective elimination of ethane. We have shown that use of the tetradentate ligand N4 promotes facile oxidation of the corresponding (N4)Pd^{II}Me₂ complex by O₂ or peroxides to generate a stable Pd^{III} intermediate followed by formation of ethane and a Pd^{II} monomethyl hydroxo complex. Cyclic voltammetry studies and use of the DMPO spin trap provide strong evidence for an inner-sphere mechanism for Pd^{II} oxidation by O₂ to form a Pd^{III}-superoxide transient intermediate. Use of cumene hydroperoxide as a mechanistic probe suggests a heterolytic O–O bond cleavage and a two-electron oxidation of the Pd^{II} precursor to form a transient Pd^{IV} intermediate before generation of the detected [(N4)-Pd^{III}Me₂]⁺ species. Notably, the C–C bond formation reactivity of the Pd^{III} complex is not affected by light or the TEMPO radical trap, as expected for a nonradical mechanism. Crossover reactivity studies of ethane formation from either the Pd^{II} precursors or the isolated Pd^{III} complexes are consistent with formation of a transient Pd^{IV} intermediate through a methyl group transfer during the C–C bond formation mechanism. Finally, the Pd^{II} monomethyl hydroxo complex formed upon ethane elimination was shown to react with

weakly acidic C–H bonds of acetone and terminal alkynes and lead to formation of a new Pd^{III}–C bond.

Overall, these results provide evidence that (N4)Pd systems can undergo aerobic oxidation, C–C bond formation, and C–H bond activation reactions, and thus could be involved in a catalytic cycle for the oxidative coupling of C–H bonds using green oxidants such as O₂. Our studies suggest the use of tetradentate ligands can promote the aerobic oxidation of organometallic Pd^{II} complexes by lowering their oxidation potential and stabilizing the generated Pd^{III} species, while also allowing the formation of transient Pd^{IV} intermediates that undergo facile reductive elimination and C–C bond formation. Our current research efforts aim to provide further insights into catalyst design for the oxidative coupling of C–H bonds using molecular oxygen as the oxidant, as well as survey the scope of this unique oxidative reactivity.

ASSOCIATED CONTENT

Supporting Information

Detailed experimental details, spectroscopic characterization, and X-ray crystallographic data. This material is available free of charge via the Internet at <http://pubs.acs.org>.

AUTHOR INFORMATION

Corresponding Author

mirica@wustl.edu

ACKNOWLEDGMENTS

We thank the Department of Chemistry at Washington University for startup funds, and the American Chemical Society Petroleum Research Fund (49914-DNI3) and DOE Catalysis Science Program (DE-FG02-11ER16254) for support. We also thank Stephanie Tucker for help with the Amplex red/HRP assay and Ying Zhang for ESI-MS analyses.

REFERENCES

- (1) (a) Negishi, E. *Handbook of Organopalladium Chemistry for Organic Synthesis*; John Wiley & Sons: Hoboken, NJ, 2002; (b) van Leeuwen, P. W. N. M. *Homogeneous Catalysis: Understanding the Art*; Kluwer Academic Publishers: Dordrecht, 2004.
- (2) (a) Miyaura, N.; Suzuki, A. *Chem. Rev.* **1995**, *95*, 2457. (b) Hartwig, J. F. *Organotransition Metal Chemistry: From Bonding to Catalysis*; University Science Books: Sausalito, 2010.
- (3) (a) Stuart, D. R.; Fagnou, K. *Science* **2007**, *316*, 1172. (b) Yeung, C. S.; Dong, V. M. *Chem. Rev.* **2011**, *111*, 1215.
- (4) (a) Stahl, S. S. *Angew. Chem., Int. Ed.* **2004**, *43*, 3400. (b) Stoltz, B. M. *Chem. Lett.* **2004**, *33*, 362. (c) Gligorich, K. M.; Sigman, M. S. *Chem. Commun.* **2009**, 3854. (d) Izawa, Y.; Stahl, S. S. *Adv. Synth. Catal.* **2010**, *352*, 3223. (e) Campbell, A. N.; Meyer, E. B.; Stahl, S. S. *Chem. Commun.* **2011**, *47*, 10257.
- (5) (a) Hull, K. L.; Lanni, E. L.; Sanford, M. S. *J. Am. Chem. Soc.* **2006**, *128*, 14047. (b) Canty, A. J. *J. Chem. Soc., Dalton Trans.* **2009**, 10409. (c) Chen, X.; Engle, K. M.; Wang, D.-H.; Yu, J.-Q. *Angew. Chem., Int. Ed.* **2009**, *48*, 5094. (d) Daugulis, O.; Do, H.-Q.; Shabashov, D. *Acc. Chem. Res.* **2009**, *42*, 1074. (e) Muniz, K. *Angew. Chem., Int. Ed.* **2009**, *48*, 9412. (f) Lyons, T. W.; Sanford, M. S. *Chem. Rev.* **2010**, *110*, 1147. (g) Sehnal, P.; Taylor, R. J. K.; Fairlamb, I. J. S. *Chem. Rev.* **2010**, *110*, 824.
- (6) Powers, D. C.; Ritter, T. *Top. Organomet. Chem.* **2011**, *35*, 129.
- (7) (a) Deprez, N. R.; Sanford, M. S. *Inorg. Chem.* **2007**, *46*, 1924. (b) Engle, K. M.; Mei, T. S.; Wang, X. S.; Yu, J. Q. *Angew. Chem., Int. Ed.* **2011**, *50*, 1478.
- (8) Lanci, M. P.; Remy, M. S.; Kaminsky, W.; Mayer, J. M.; Sanford, M. S. *J. Am. Chem. Soc.* **2009**, *131*, 15618.

- (9) An early study reported that presence of O₂ leads to faster oxidation of a Pd^{II} complex to form a Pd^{III} species: McAuley, A.; Whitcombe, T. W. *Inorg. Chem.* **1988**, *27*, 3090.
- (10) Chuang, G. J.; Wang, W.; Lee, E.; Ritter, T. J. *Am. Chem. Soc.* **2011**, *133*, 1760.
- (11) (a) Zhang, J.; Khaskin, E.; Anderson, N. P.; Zavalij, P. Y.; Vedernikov, A. N. *Chem. Commun.* **2008**, 3625. (b) Boisvert, L.; Denney, M. C.; Kloek, H. S.; Goldberg, K. I. *J. Am. Chem. Soc.* **2009**, *131*, 15802.
- (12) (a) Zhang, Y.-H.; Yu, J.-Q. *J. Am. Chem. Soc.* **2009**, *131*, 14654. (b) Wang, A.; Jiang, H.; Chen, H. *J. Am. Chem. Soc.* **2009**, *131*, 3846. (c) Zhu, M.-K.; Zhao, J.-F.; Loh, T.-P. *J. Am. Chem. Soc.* **2010**, *132*, 6284.
- (13) Khusnutdinova, J. R.; Rath, N. P.; Mirica, L. M. *J. Am. Chem. Soc.* **2010**, *132*, 7303.
- (14) Che, C. M.; Li, Z. Y.; Wong, K. Y.; Poon, C. K.; Mak, T. C. W.; Peng, S. M. *Polyhedron* **1994**, *13*, 771.
- (15) Drew, D.; Doyle, J. R. *Inorg. Synth.* **1990**, *28*, 346.
- (16) Meneghetti, S. P.; Lutz, P. J.; Kress, J. *Organometallics* **2001**, *20*, 5050.
- (17) See the Supporting Information.
- (18) Detailed electrochemical studies of these complexes will be published elsewhere.
- (19) Sarneski, J. E.; McPhail, A. T.; Onan, K. D.; Erickson, L. E.; Reilley, C. N. *J. Am. Chem. Soc.* **1977**, *99*, 7376.
- (20) Wieghardt, K.; Koeppe, M.; Swiridoff, W.; Weiss, J. *J. Chem. Soc., Dalton Trans.* **1983**, 1869.
- (21) Rostovtsev, V. V.; Henling, L. M.; Labinger, J. A.; Bercaw, J. E. *Inorg. Chem.* **2002**, *41*, 3608.
- (22) (a) Blake, A. J.; Gordon, L. M.; Holder, A. J.; Hyde, T. I.; Reid, G.; Schröder, M. *J. Chem. Soc., Chem. Commun.* **1988**, 1452. (b) Blake, A. J.; Holder, A. J.; Roberts, Y. V.; Lavery, A. J.; Schröder, M. *J. Organomet. Chem.* **1987**, *323*, 261.
- (23) Stephen, E.; Huang, D.; Shaw, J. L.; Blake, A. J.; Collison, D.; Davies, E. S.; Edge, R.; Howard, J. A. K.; McInnes, E. J. L.; Wilson, C.; Wolowska, J.; McMaster, J.; Schröder, M. *Chem.—Eur. J.* **2011**, *17*, 10246.
- (24) (a) Prokopchuk, E. M.; Jenkins, H. A.; Puddephatt, R. J. *Organometallics* **1999**, *18*, 2861. (b) Prokopchuk, E. M.; Puddephatt, R. J. *Can. J. Chem.* **2003**, *81*, 476.
- (25) (a) Vedernikov, A. N.; Binfield, S. A.; Zavalij, P. Y.; Khusnutdinova, J. R. *J. Am. Chem. Soc.* **2006**, *128*, 82. (b) Khusnutdinova, J. R.; Zavalij, P. Y.; Vedernikov, A. N. *Organometallics* **2007**, *26*, 2402.
- (26) The ratio of **3** to ethane remains close to 2:1 at the initial period of reaction and slightly decreases with time, presumably due to slow decomposition of **3** (Table S1).
- (27) (a) Stahl, S. S.; Thorman, J. L.; Nelson, R. C.; Kozee, M. A. *J. Am. Chem. Soc.* **2001**, *123*, 7188. (b) Konnick, M. M.; Guzei, I. A.; Stahl, S. S. *J. Am. Chem. Soc.* **2004**, *126*, 10212. (c) Sigman, M. S.; Jensen, D. R. *Acc. Chem. Res.* **2006**, *39*, 221. (d) Cai, X.-C.; Majumdar, S.; Fortman, G. C.; Cazin, C. S. J.; Slawin, A. M. Z.; Lhermitte, C.; Prabhakar, R.; Germain, M. E.; Palluccio, T.; Nolan, S. P.; Rybak-Akimova, E. V.; Temprado, M.; Captain, B.; Hoff, C. D. *J. Am. Chem. Soc.* **2011**, *133*, 1290.
- (28) (a) Pieri, G.; Pasquali, M.; Leoni, P.; Englert, U. *J. Organomet. Chem.* **1995**, *491*, 27. (b) Dura-Vila, V.; Mingos, D. M. P.; Vilar, R.; White, A. J. P.; Williams, D. J. *Chem. Commun.* **2000**, 1525. (c) Huacuja, R.; Graham, D. J.; Fafard, C. M.; Chen, C.-H.; Foxman, B. M.; Herbert, D. E.; Alliger, G.; Thomas, C. M.; Ozerov, O. V. *J. Am. Chem. Soc.* **2011**, *133*, 3820. (d) Denney, M. C.; Smythe, N. A.; Cetto, K. L.; Kemp, R. A.; Goldberg, K. I. *J. Am. Chem. Soc.* **2006**, *128*, 2508.
- (29) (a) Bianchi, D.; Bortolo, R.; D'Aloisio, R.; Ricci, M. *Angew. Chem., Int. Ed.* **1999**, *38*, 706. (b) Bianchi, D.; Bortolo, R.; D'Aloisio, R.; Ricci, M. *J. Mol. Catal. A: Chem.* **1999**, *150*, 87.
- (30) The formation of H₂O₂ catalyzed by Pd^{II} cannot be excluded at the later stages of the reaction, as volumetric measurements indicate that after initial absorption of 0.3–0.5 equiv of O₂, a slower consumption of O₂ continues even after the complete conversion of **1** (see Supporting Information).
- (31) (a) Sawyer, D. T.; Chiericato, G.; Angelis, C. T.; Nanni, E. J.; Tsuchiya, T. *Anal. Chem.* **1982**, *54*, 1720. (b) Anson, F. C.; Shi, C.; Steiger, B. *Acc. Chem. Res.* **1997**, *30*, 437. (c) McCrory, C. C. L.; Ottenwaelder, X.; Stack, T. D. P.; Chidsey, C. E. D. *J. Phys. Chem. A* **2007**, *111*, 12641.
- (32) (a) Zhang, J.; Anson, F. C. *Electrochim. Acta* **1993**, *38*, 2423. (b) Lei, Y.; Anson, F. C. *Inorg. Chem.* **1994**, *33*, 5003. (c) Lei, Y.; Anson, F. C. *Inorg. Chem.* **1995**, *34*, 1083.
- (33) (a) Buettner, G. R. *Free Radical Biol. Med.* **1987**, *3*, 259. (b) Reszka, K.; Chignell, C. F. *Free Radical Res. Commun.* **1991**, *14*, 97.
- (34) (a) Hamilton, D. E.; Drago, R. S.; Telser, J. *J. Am. Chem. Soc.* **1984**, *106*, 5353. (b) Furutachi, H.; Fujinami, S.; Suzuki, M.; Okawa, H. *J. Chem. Soc., Dalton Trans.* **2000**, 2761.
- (35) Lamour, E.; Routier, S.; Bernier, J.-L.; Catteau, J.-P.; Bailly, C.; Vezin, H. *J. Am. Chem. Soc.* **1999**, *121*, 1862.
- (36) The detailed reactivity studies of these complexes will be published elsewhere.
- (37) (a) Matsui, T.; Nagano, S.; Ishimori, K.; Watanabe, Y.; Morishima, I. *Biochemistry* **1996**, *35*, 13118. (b) Matsui, T.; Ozaki, S.-I.; Watanabe, Y. *J. Am. Chem. Soc.* **1999**, *121*, 9952. (c) Coggins, M. K.; Kovacs, J. A. *J. Am. Chem. Soc.* **2011**, *133*, 12470.
- (38) Yamazaki, I.; Piette, L. H. *J. Biol. Chem.* **1990**, *265*, 13589.
- (39) (a) Canty, A. J.; Jin, H.; Roberts, A. S.; Skelton, B. W.; White, A. H. *Organometallics* **1996**, *15*, 5713. (b) Oloo, W.; Zavalij, P. Y.; Zhang, J.; Khaskin, E.; Vedernikov, A. N. *J. Am. Chem. Soc.* **2010**, *132*, 14400.
- (40) Alsters, P. L.; Teunissen, H. T.; Boersma, J.; Spek, A. L.; van Koten, G. *Organometallics* **1993**, *12*, 4691.
- (41) Consumption of slightly more than 0.5 equivalent of cumene hydroperoxide after 8 h may be due to slow decomposition of cumene hydroperoxide in the presence of **3** (see Supporting Information).
- (42) (a) Rebbert, R. E.; Ausloos, P. *J. Phys. Chem.* **1962**, *66*, 2253. (b) Lyon, R. K.; Levy, D. H. *J. Am. Chem. Soc.* **1961**, *83*, 4290.
- (43) (a) Byers, P. K.; Canty, A. J.; Skelton, B. W.; White, A. H. *J. Chem. Soc., Chem. Commun.* **1986**, 1722. (b) Byers, P. K.; Canty, A. J.; Crespo, M.; Puddephatt, R. J.; Scott, J. D. *Organometallics* **1988**, *7*, 1363.
- (44) Byers, P. K.; Canty, A. J.; Skelton, B. W.; White, A. H. *J. Chem. Soc., Chem. Commun.* **1987**, 1093.
- (45) (a) Seligson, A. L.; Troglor, W. C. *J. Am. Chem. Soc.* **1992**, *114*, 7085. (b) Johansson, L.; Ryan, O. B.; Romming, C.; Tilset, M. *Organometallics* **1998**, *17*, 3957.
- (46) Aye, T.-K.; Canty, A. J.; Crespo, M.; Puddephatt, R. J.; Scott, J. D.; Watson, A. A. *Organometallics* **1989**, *8*, 1518.
- (47) Klein, A.; Dogan, A.; Feth, M.; Bertagnolli, H. *Inorg. Chim. Acta* **2003**, *343*, 189.
- (48) (a) Yang, G.; Miao, R.; Li, Y.; Hong, J.; Zhao, C.; Guo, Z.; Zhu, L. *Dalton Trans.* **2005**, 1613. (b) Cao, L.; Jennings, M. C.; Puddephatt, R. J. *Dalton Trans.* **2009**, 5171.
- (49) (a) Yoshida, T.; Okano, T.; Otsuka, S. *J. Chem. Soc., Dalton Trans.* **1976**, 993. (b) Grushin, V. V.; Bensimon, C.; Alper, H. *Organometallics* **1993**, *12*, 2737. (c) Fulton, J. R.; Holland, A. W.; Fox, D. J.; Bergman, R. G. *Acc. Chem. Res.* **2002**, *35*, 44. (d) Bercaw, J. E.; Hazari, N.; Labinger, J. A.; Oblad, P. F. *Angew. Chem., Int. Ed.* **2008**, *47*, 9941. (e) Williams, T. J.; Caffyn, A. J. M.; Hazari, N.; Oblad, P. F.; Labinger, J. A.; Bercaw, J. E. *J. Am. Chem. Soc.* **2008**, *130*, 2418.
- (50) Remy, M. S.; Cundari, T. R.; Sanford, M. S. *Organometallics* **2010**, *29*, 1522.
- (51) (a) Feng, Y.; Lail, M.; Barakat, K. A.; Cundari, T. R.; Gunnoe, T. B.; Petersen, J. L. *J. Am. Chem. Soc.* **2005**, *127*, 14174. (b) Tenn, W. J.; Young, K. J. H.; Bhalla, G.; Oxgaard, J.; Goddard, W. A.; Periana, R. A. *J. Am. Chem. Soc.* **2005**, *127*, 14172. (c) Tenn, W. J.; Young, K. J. H.; Oxgaard, J.; Nielsen, R. J.; Goddard, W. A.; Periana, R. A. *Organometallics* **2006**, *25*, 5173. (d) Kloek, S. M.; Heinekey, D. M.; Goldberg, K. I. *Angew. Chem., Int. Ed.* **2007**, *46*, 4736. (e) Hanson, S. K.; Heinekey, D. M.; Goldberg, K. I. *Organometallics* **2008**, *27*, 1454.
- (52) (a) Maitra, A. M. *Appl. Catal., A* **1993**, *104*, 11. (b) Liu, S.; Tan, X.; Li, K.; Hughes, R. *Cat. Rev.: Sci. Eng.* **2001**, *43*, 147.